2.8 FRICTION STIR WELDING OF ODS STEELS AND ADVANCED FERRITIC STRUCTURAL STEELS

— Z. Feng, W. Tang, X. Yu, G. Chen, D. Hoelzer, and L. Tan (Oak Ridge National Laboratory)

OBJECTIVE

This project addresses the critical technology gap of joining oxide dispersion strengthened (ODS) steels, nanostructured ferritic alloys (NFAs), reduced-activation ferritic/martensitic (RAFM) steels, and dissimilar metal joints of ODS/NFAs and RAFM steels through friction stir welding (FSW) technology. The research focuses on understanding the stability of the strengthening phases in the weld region, and the bonding mechanisms between dissimilar structural steels as a function of FSW process conditions.

Specific project objectives are (i) developing the process parameter space to consistently produce defect-free welds of the same and dissimilar metals, (ii) developing the knowledge base and practical applicable approaches to tailor and optimize the microstructure features in the weld to match the properties of the base metal through process innovation, and (iii) producing representative weld joints and welded components to support future testing and evaluation at high temperature and irradiation environments in collaboration with JAEA and other international teams.

SUMMARY

For this final reporting period of the project, the baseline FSW process conditions for joining ODS steels and RAFM steels have been successfully developed. A computational fluid dynamics (FCD) based model has been developed and applied to understand of temperature and material flow during FSW of these advanced structural materials. A unique high temperature digital image correlation (DIC) strain measurement technique enabled experimentally determining the local deformation behavior in different regions of FSW of RAFM steel in high temperature creep test. The DIC measurement revealed drastic increase in creep resistance (i.e. reduced creep rate) in the stir zone, and reduced creep resistance in the heat affected zone (HAZ), an area requiring further process optimization. Finally, the sizes of the oxides/nano-cluster features, the primary strengthening phase in ODS alloys, is highly dependent on the FSW process conditions. This shows the feasibility of using FSW to join advanced fusion structural materials with better than base metal properties.

PROGRESS AND STATUS

Microstructure characterization of the dissimilar materials ODS alloy and RAFM steel FSW joint

A defect-free dissimilar materials joint between 14YWT and 9Cr advanced steels was produced by friction stir welding (FSW) and was reported previously. Both alloys were developed and produced at Oak Ridge National Laboratory (ORNL). Optical microstructures in various metallurgical zones of the dissimilar materials joint were also reported. Though optical images of the weld confirmed the joint was free of defects, detailed grain structures and hardening precipitates, which are important strengthening factors, are need to be characterized to further evaluate the joint quality.

In this period of study, we concentrated on examining the microstructure of this dissimilar materials joint using scanning electron microscope (SEM). Three regions on the 14YWT side, including stir zone (SZ), heat affected zone (HAZ) and base metal (BM) were characterized in details. Backscattered electron images of the ODS alloy 14YWT BM, SZ and HAZ are shown in Figure 1. In the SZ of 14YWT, significant grain growth was observed. Grain size of SZ is about 5-10 microns compared to 0.3 microns in base metal (BM). In addition, the HAZ also exhibits grain growth (grain size is about 1-2 microns) due to the heat introduced by friction stir process.

Figure 2 shows backscatter electron images of SZ and BM. For BM, most of the precipitates were not resolved by SEM since these precipitates are on the order of 2-5nm (nano-clusters). Only sub-micron ferritic grains were observed in BM. In SZ, t*he “bright” precipitates inside grains indicate they are enriched with greater atomic number elements. As a result, these precipitates could be oxides enriched

with Y and Ti, which need to be confirmed by further atom probe tomography or transmission electron microscopy.

In our study reported in previous reporting periods, it was found that FSW can preserve the nano-size precipitates in 14YWT. Similar phenomenon was also observed in the current report. Precipitates were observed in SZ.

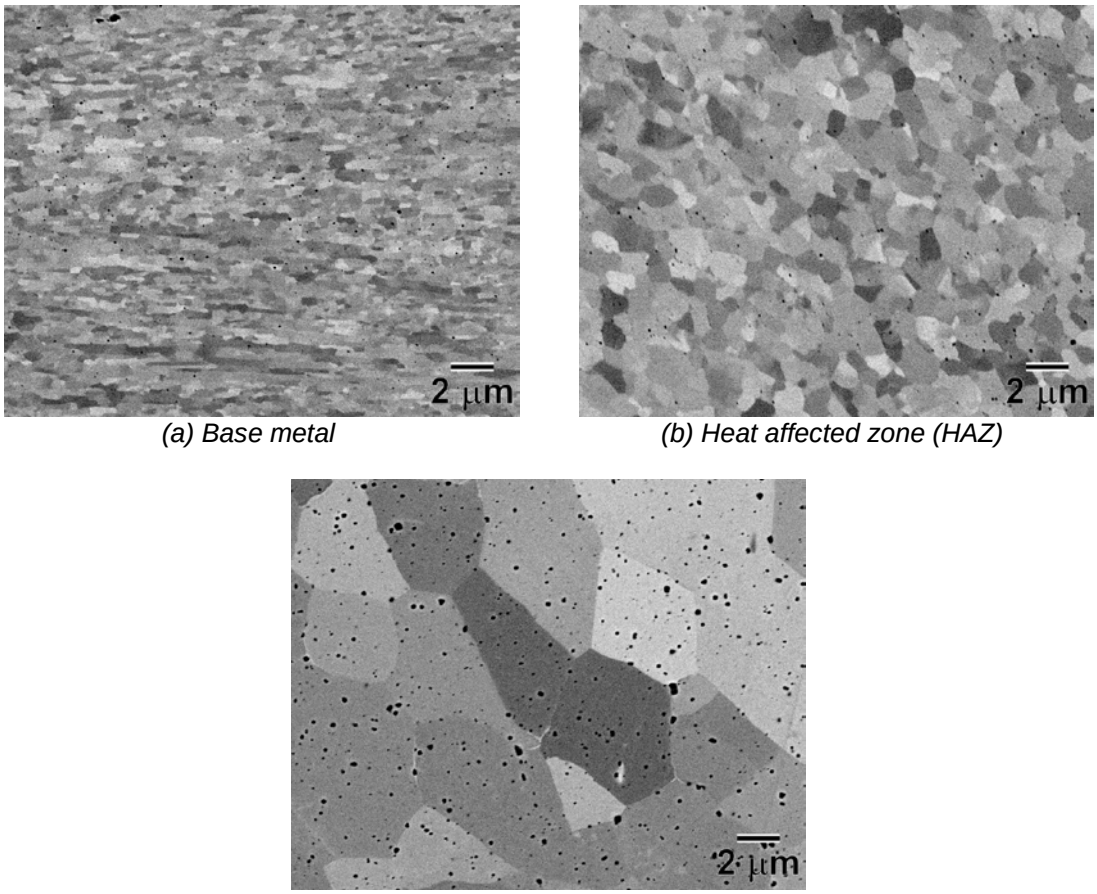

(a) Base metal *(b) Heat affected zone (HAZ)*

(c) Stir zone (SZ)

Figure 1. Electron backscatter images of 14YWT at various metallurgical zones

In the SZ, the interface between 9Cr and 14YWT also studied. Figure 3 shows backscattered electron image of 9Cr/14YWT interface. Ferrite grains 14YWT near the interface are elongated. The elongated grains are due to great deformation introduced by FSW. In addition, voids were observed in 9Cr steel adjacent to the interface, but not in 14YWT. The voids are in the size of 1-3 microns and mainly locate at the 9Cr prior austenite grain boundaries. The presence of the voids is on consistent along the interface. Some regions in 9Cr adjacent to the interface were free of voids (in the center of Figure 3a). Possible reasons for those voids appearance include the FSW tool wear effect and base metal precipitates etching effect. FSW of high temperature materials is very harsh to the FSW tool due to the elevated welding temperature (it can reach to 1000 °C easily) and high reaction forces. In another study of FSW stainless steel, voids were observed in certain regions of the joint stir zone after polycrystalline cubic boron nitride (PCBN) FSW tool was worn. The tool geometry change, features change and particles falling off from the tool may result voids in SZ. Meanwhile, the 9Cr base metal contains a couple of micrometer sizes particles, which are shown in Figure 4. It is possible that those particles were preferentially etched by the chemical etchant.

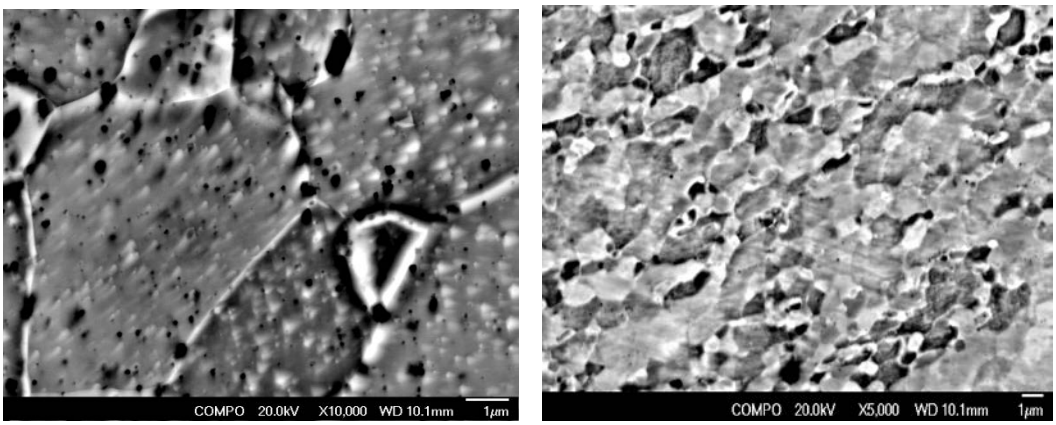

(a) 14YWT stir zone *(b) 14YWT base metal*

Figure 2. Grain and precipitates growth in the 14YWT SZ after FSW

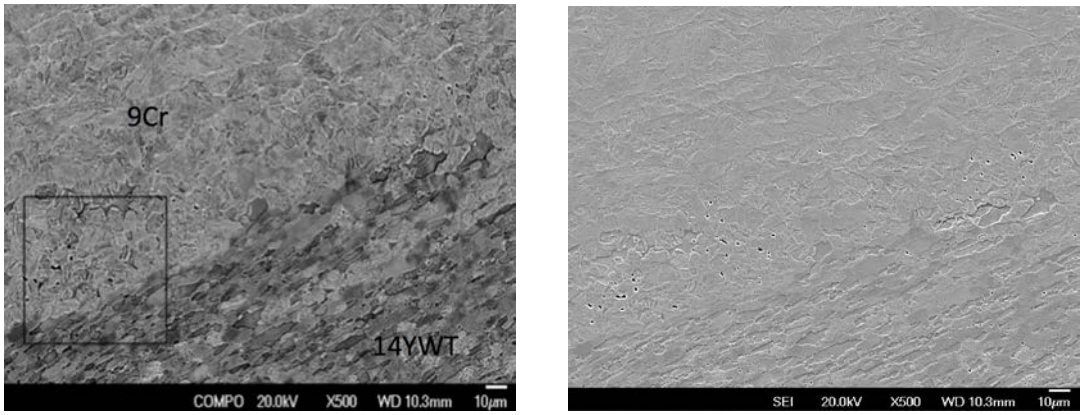

(a) backscattered electron imaged *(b) Secondary electron image*

Figure 3. *Image of 9Cr/14YWT interface showing voids at 9Cr prior austenite grain boundaries*

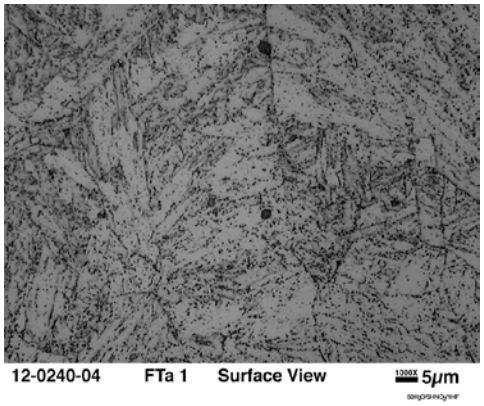

Figure 4. Micron size particles in 9Cr base metal

High temperature creep testing and characterization of RAFM friction stir welded joints

RAFM steel F82H was joined by FSW previously. Optical microscopy results as well as microhardness distributions of the welded joint were reported.

Cross-weld creep tests were performed on F82H FSW joints. Round bar specimens were machined out from the F82H FSW joint perpendicular to the welding direction for tensile creep-rupture test. The weld zone was located in the middle of each specimen. Specimens were machined to 6 mm diameter with a gage length of 40 mm, as shown in Figure 5. A unique feature of our creep test was the use of digital image correlation (DIC) technique to study the anticipated non-uniform deformation and creep behavior in the cross-weld specimen, due to the fact of the highly non-uniform microstructure gradient in the SZ and HAZ region. Before the creep test, special high-temperature random speckle pattern was applied on the specimen surface for DIC measurement of local deformation. Thermocouples were attached to the specimen to record the testing temperature.

Figure 5. Tensile creep-rupture specimens

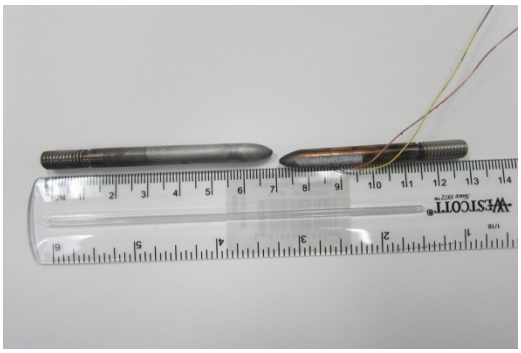

Figure 6. Broken tensile creep-rupture specimen

Tensile creep-rupture tests of welded joints were performed using a Gleeble™ thermal mechanical simulator. Two test temperatures were chosen, 550°C and 650°C, which are typical temperatures for nuclear structural materials application. The sample was heated to 550°C or 650°C at 5°C/s, and a constant stress of 100 MPa was applied during the creep test.

For the sample tested at 650°C, it failed after 16 hours of testing. Post-test analysis showed that the failure location was in FSW HAZ, and the broken specimen is shown in Figure 6. Traverse creep strain across the sample from DIC analysis 5 minutes before fracture is shown in Figure 7. From Figure 7, clearly the strain peak value is located at the HAZ and the strain valley is located in the FSW stir zone. Therefore, high temperature creep plastic deformation was concentrated in the HAZ of the welded joint and the stir zone plastic deformation was even lower than that in the base metal.

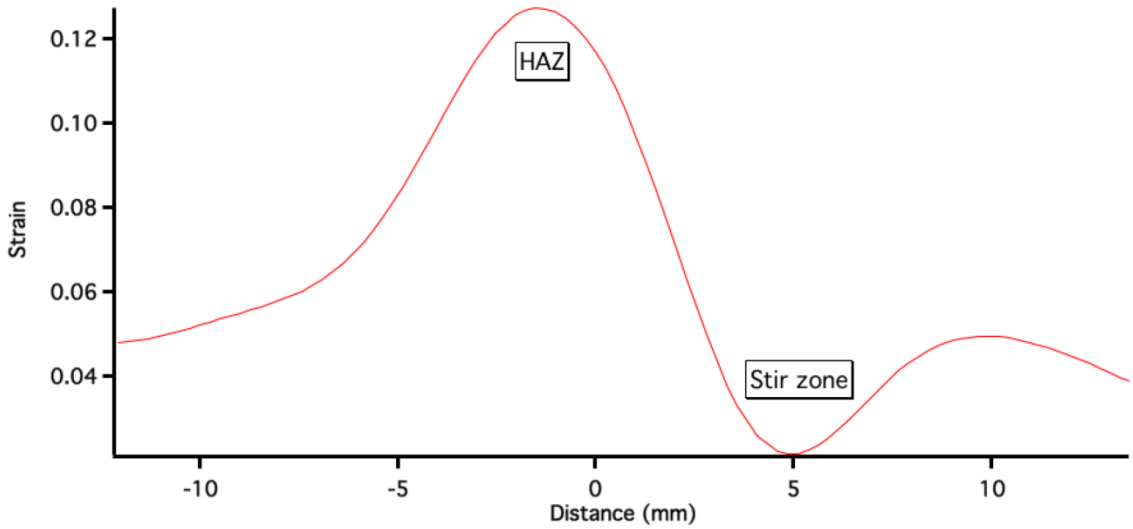

Figure 7. Traverse creep strain distribution of the sample tested at 650°C before fracture

The stress-rupture test at 550°C was interrupted at 89 hours, and the specimen didn't show obvious deformation or necking. After the stress-rupture test, the strain histories of SZ, HAZ and BM were plotted in Figure 8. In general, the system error of current DIC strain measurement is less than 3 X 10^{-4}. Before the loading in creep testing, HAZ and BM showed strain of 0.0083 and SZ showed strain of 0.0070. Those strains were thermal strains at 550°C. When stress was applied, the sample started to creep with time went by but there were almost no creep deformation in SZ at all. For BM, the secondary creep started at about 10.2 hours and the secondary creep rate was 2.9 X10^{-5} /h. For HAZ, the secondary creep started early at about 2.5 hours and the secondary creep rate was 4.8X10^{-5} /h. For SZ, creep strain should be less than 3 X 10^{-4} (system error of DIC). Assume the creep strain is 3 X 10^{-4}, which result in creep rate of 3.4 X10^{-6}/h. In general, the secondary creep rate in HAZ of a fusion welded ferritic steel joint is almost 5 times higher than that in BM. However, the secondary creep rate in HAZ is only about 1.7 times higher than that in BM for current friction stir welded RAFM joint.

Stress vs. creep rate was plotted in Figure 9. The base metal creep behavior follows Norton's power law. For HAZ, creep rate is only slightly above the power law curve. However, creep rate of SZ is significant lower than power law curve. The stir zone is expected to have much better creep resistance than base material.

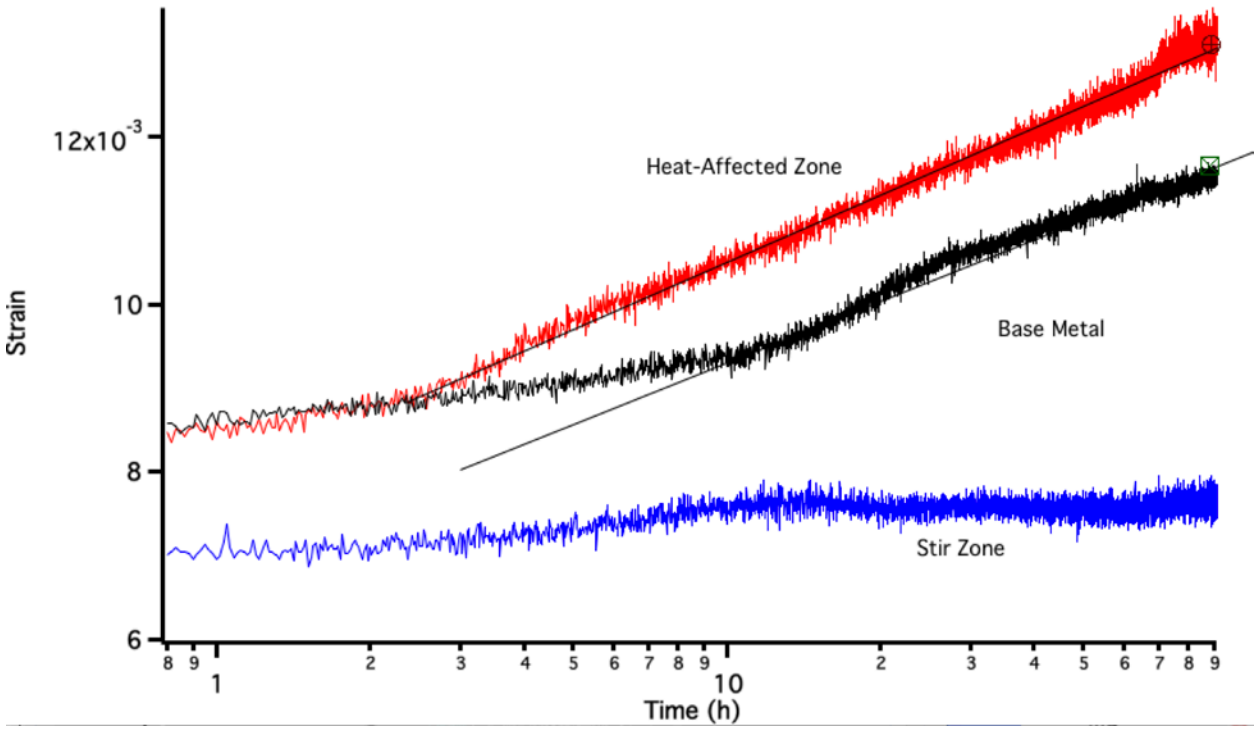

Figure 8. Strain vs. time for BM, SZ and HAZ of a RAFM FSW joint in creep-rupture test.

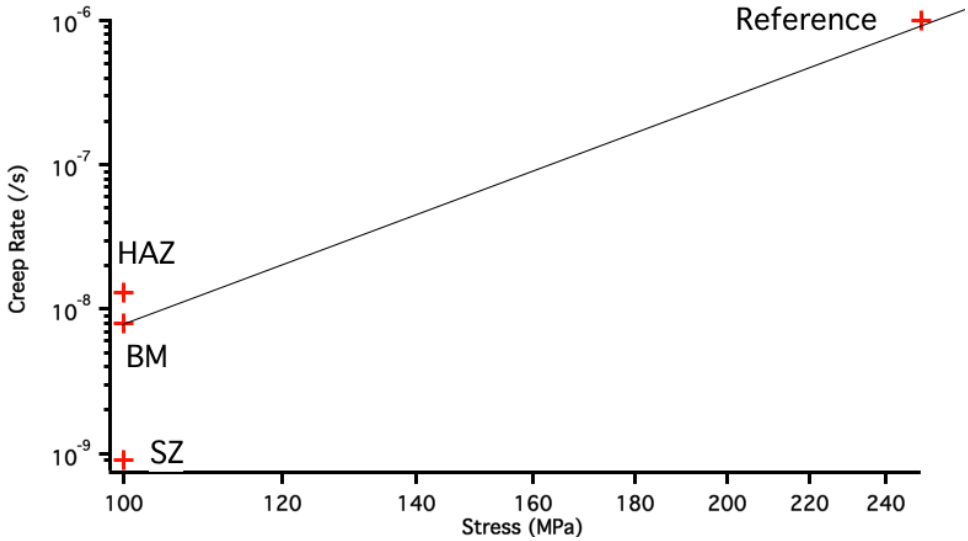

Figure 9. Stress vs. strain rate for different regions of the friction stir weld

Friction-induced material behavior in FSW thermal-mechanical coupled computer modeling

Fundamental studies of thermal-mechanical conditions, such as temperature, strain and strain rate, in FSW of ODS and RAFM steels were carried out by 3D thermally-mechanically coupled numerical models developed based on Computational Fluid Dynamics (CFD). Reasonable FSW temperature fields and material flow patterns were obtained by using the computer models developed in last year. This period of

study was focused on enhancing the developed numerical models, in order to predict the thermal-mechanical conditions in wide range of welding parameters, which facilities the understanding of material behaviors in different welding conditions. The temperature dependency of material flow strength is critical in predicting the variations of heat generation, temperature and material flow in different conditions owing to the thermal-mechanical nature of FSW process. The numerical modeling in this period of study was enhanced by taking into consideration of material flow stresses measured at various elevated temperatures from publications. The enhanced computer models were used to simulate the material behavior in different conditions. Various modeling conditions and parameters in the simulations are shown in Table 1. By applying those conditions and parameters, different FSW temperature distributions are obtained from modeling results and they are shown in Figure 10. From Figure 10, it is obvious that the welding temperature of 400 rpm FSW is higher than austenite phase transformation temperature while that of 100 rpm FSW processes is around the austenite phase transformation temperature value for the modeled material Eurofer 97 RAFM steel (A_{c1b} = 820 °C and A_{c1e} = 890 °C). In FSW, the peak temperature is mainly affected by welding power input and welding power input is mainly affected by FSW tool rotating rate. From the previous experimental results, martensitic was the major grain microstructure in 400 rpm condition FSW stir zone, and partially martensitic microstructure was observed in 100 rpm condition FSW stir zone. The modeling results of FSW temperature fields evolved the reason behind those experimental results.

Table 1. Parameters in the computation

Tool rotation rate/ rpm	Welding speed/ ipm	Magnitude of frictional stress between tool and workpiece/ MPa
100	2.0	15.0~25.0
200	2.0	15.0~25.0
400	2.0	15.0~25.0

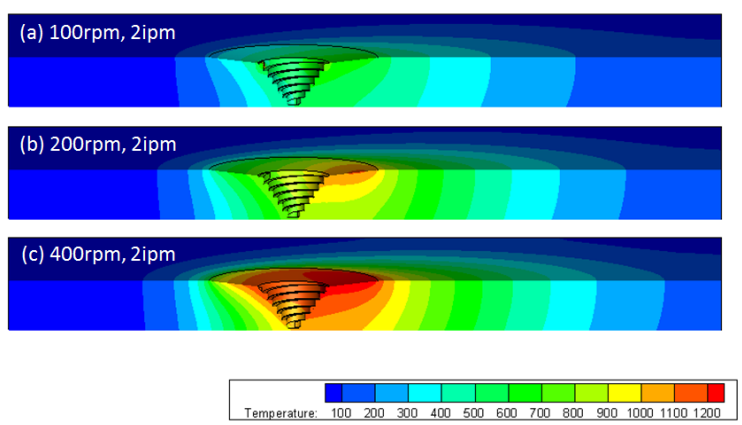

Figure 10. Temperature fields with different welding parameters from computer modeling.

Fundamentally, the FSW joint properties are highly depended on its thermal – mechanical history during the welding process, but lots of the thermal – mechanical information will not show after the FSW because of materials recovering and recrystallization. Based on the numerical simulating development, the thermal-mechanical history of material deposited in the weld is studied by particle tracing to obtain material deformation facts. The distributions of plastic strain and peak temperature at a FSW joint cross section are shown in Figure 11. It is clear that plastic strain and peak temperature distributed inside the stir zone unevenly, and that explains stir zone grain size and microstructure dissimilarities in metallographic study.

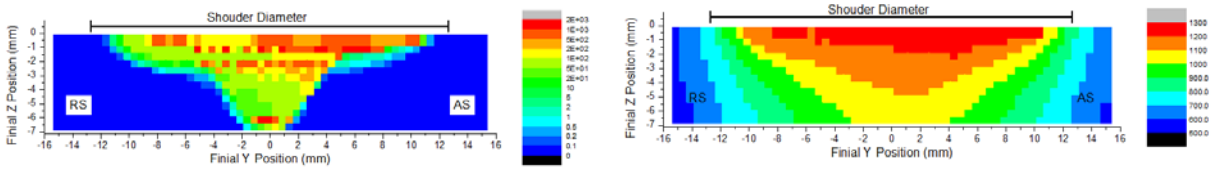

(a) Strain distribution. *(b) Peak temperature distribution.*

Figure 11. Plastic strain and peak temperature distribution at a cross section in FSW

Conclusions

1. Although FSW is a solid state low heat input joining technology, it still caused grain structures and strengthening precipitates growth inside the stir zone with parameters applied in this study. Further investigation is needed to suppress the grain and precipitates grown by adjusting FSW conditions and parameters.
2. The HAZ of a RAFM steel FSW joint is the weakest point to resist high temperature creep, and that of the stir zone is the strongest, even better than the base metals.
3. The 3D thermal – mechanical coupled computer modeling provides excellent information for fundamental understanding of the FSW process.

Future Work

We have successfully completed this project.